Dynamical approach to spectator fragmentation in Au+Au reactions at 35 MeV/A

Yogesh K. Vermani and Rajeev K. Puri Department of Physics, Panjab University, Chandigarh -160 014, India (Dated: November 6, 2018)

The characteristics of fragment emission in peripheral $^{197}\mathrm{Au} + ^{197}\mathrm{Au}$ collisions 35 MeV/A are studied using the two clusterization approaches within framework of quantum molecular dynamics model. Our model calculations using minimum spanning tree (MST) algorithm and advanced clusterization method namely simulated annealing clusterization algorithm (SACA) showed that fragment structure can be realized at an earlier time when spectators contribute significantly toward the fragment production even at such a low incident energy. Comparison of model predictions with experimental data reveals that SACA method can nicely reproduce the fragment charge yields and mean charge of the heaviest fragment. This reflects suitability of SACA method over conventional clusterization techniques to investigate spectator matter fragmentation in low energy domain.

PACS numbers: 25.70.-z 25.70.Mn 24.10.Lx

I. INTRODUCTION

The study of heavy-ion (HI) reactions at intermediate energies provides an important platform to probe the highly non-equilibrium environment produced in the reaction zone as well as properties of excited fragments evolved from the spectator zone [1–5]. The spectator matter fragmentation at relativistic bombarding energies is also characterized by a rise and fall pattern [1–3, 5]. These experiments performed on ALADiN set-up mainly focussed on the liquid-gas phase transitions [3–6] and universality behavior observed in the fragment-emission at incident energies > 400 MeV/A [2, 5]. The clusterization approach based upon minimization of fragments' total energy dubbed as simulated annealing clusterization algorithm (SACA) is reported to explain this rise and fall trend in the multiplicity of IMFs with collision geometry quite accurately at relativistic bombarding energies [7]. Conventional clusterization approach based upon spatial correlation among nucleons, however, failed completely to explain higher IMF yields at large impact parameters [7, 8].

The reaction dynamics and associated non-equilibrium aspects in low-energy HI collisions are, however, still poorly understood phenomena [9, 10]. The important question associated with this domain is whether nuclear system can reach thermal equilibrium before break-up or not [11]. Most of nucleon-nucleon collisions are Pauli blocked and mean field governs the reaction dynamics in low energy domain [12–14]. In case of peripheral collisions, we have projectile-like and target-like remnants and fusion-fission events dominate the scenario. The fusion events disappear as the incident energy increases marked by the onset of multifragmentation. In the low energy range (i.e. between 40 and 70 MeV/A), a significant fraction of the intermediate mass fragments originates from mid-velocity region [9]. This type of preequilibrium emission has been conjectured as 'extended neck' emission due to the dynamical fluctuations that increase with the incident energy. Many experiments have indicated that binary dissipative collisions (BDC) dominate the scenario in such low energy HI collisions [15]. As far as decays from quasiprojectile and quasitarget are concerned, molecular dynamics approaches coupled with conventional clusterization algorithm mayn't reproduce fragment charge yields accurately [16].

In the present paper, we aim to see whether SACA method can describe spectator matter fragmentation in low energy domain or not. The confrontation of the theoretical predictions employing advanced clusterization technique with experimental data can be of importance to understand the physical scenario behind cluster production mechanism in low-energy HI collisions. We shall compute the fragment observables for peripheral Au(35 MeV/A) + Au collisions employing MST and SACA clusterization subroutines. A comparison with experimental results recently obtained by Multics-Miniball group [17, 18] is also attempted to explore the applicability of SACA method. Section II describes the main features of the QMD model along with simulated annealing clusterization algorithm (SACA). Our results are discussed in section III and summarized in section IV.

II. THE MODEL

The quantum molecular dynamics model is A-body transport theory that incorporates the quantum features of Pauli blocking and stochastic nucleon-nucleon (n-n) scattering [14, 19]. Each nucleon in the colliding system is represented by a gaussian wave packet as [14]:

$$\psi_{i}(\mathbf{r}, \mathbf{p}_{i}(t), \mathbf{r}_{i}(t)) = \frac{1}{(2\pi L)^{3/4}} exp\left[\frac{i}{\hbar}\mathbf{p}_{i}(t) \cdot \mathbf{r} - \frac{(\mathbf{r} - \mathbf{r}_{i}(t))^{2}}{4L}\right]. \quad (1)$$

Mean position $\mathbf{r}_i(t)$ and mean momentum $\mathbf{p}_i(t)$ are the two time dependent parameters. The gaussian width has fixed value $\sqrt{L}=1.08$ fm. The centers of these

Gaussian wave packets propagate in coordinate (\mathcal{R}_3) and momentum (\mathcal{P}_3) space according to the classical equations of motion:

$$\dot{\mathbf{p}}_i = -\frac{\partial \langle \mathcal{H} \rangle}{\partial \mathbf{r}_i}; \quad \dot{\mathbf{r}}_i = \frac{\partial \langle \mathcal{H} \rangle}{\partial \mathbf{p}_i}.$$
 (2)

The Hamiltonian \mathcal{H} appearing in Eq. 2 has contribution from the local Skyrme-type, Yukawa and effective Coulomb interactions [14]. Since QMD model gives just the phase space of nucleons, one needs secondary algorithm to clusterize the phase space. The standard clusterization approach namely minimum spanning tree (MST) procedure assumes that the correlating nucleons belong to the same fragment if their inter-nucleon distance $|\mathbf{r}_i - \mathbf{r}_j|$ is smaller than 4 fm. This approach is successful when the system is dilute and clusters are well separated in \mathcal{R}_3 space.

A. The SACA formalism

This sophisticated clusterization approach allows early identification of fragments before these are well separated in coordinate space. The SACA method works on the principle of energy minimization of fragmenting system. The pre-clusters obtained with the MST method are subjected to a binding energy check [20, 21]:

$$\zeta_{i} = \frac{1}{N_{f}} \sum_{\alpha=1}^{N_{f}} \left[\sqrt{\left(\mathbf{p}_{\alpha} - \mathbf{P}_{N_{f}^{c.m.}}\right)^{2} + m_{\alpha}^{2}} - m_{\alpha} + \frac{1}{2} \sum_{\beta \neq \alpha}^{N_{f}} V_{\alpha\beta} \left(\mathbf{r}_{\alpha}, \mathbf{r}_{\beta}\right) \right] < -E_{bind}, \quad (3)$$

with $E_{bind} = 4.0 \text{ MeV}$ if $N_f \geq 3$ and $E_{bind} = 0$ otherwise. In Eq. (3), N_f is the number of nucleons in a fragment and $\mathbf{P}_{N_f}^{c.m.}$ is the center-of-mass momentum of the fragment. The requirement of a minimum binding energy excludes the loosely bound fragments which will decay at later stage. To look for the most bound configuration (MBC), we start from a random configuration which is chosen by dividing whole system into few fragments. The energy of each cluster is calculated by summing over all the nucleons present in that cluster using Eq. (3).

Let the total energy of a configuration k be $E_k (= \sum_i N_f \zeta_i)$, where N_f is the number of nucleons in a fragment and ζ_i is the energy per nucleon of that fragment. Suppose a new configuration k' (which is obtained by (a) transferring a nucleon from randomly chosen fragment to another fragment or by (b) setting a nucleon free, or by (c) absorbing a free nucleon into a fragment) has a total energy $E_{k'}$. If the difference between the old and new configuration $\Delta E (= E_{k'} - E_k)$ is negative, the new configuration is always accepted. If not, the new configuration k' may nevertheless be accepted with a probability of $\exp(-\Delta E/v)$, where v is called the control parameter.

This procedure is known as Metropolis algorithm. The control parameter is decreased in small steps. This algorithm will yield eventually the most bound configuration (MBC).

Since this combination of a Metropolis algorithm with slowly decreasing control parameter v is known as $simulated\ annealing$, so our approach is dubbed as $simulated\ annealing\ clusterization\ algorithm\ (SACA)$. For the present calculations we have employed improvised version of SACA method in which fragments are confronted against realistic binding energies instead of constant binding energy check of -4.0 MeV/nucleon [22]. It may be mentioned that this modification has nearly no effect on final fragment yields and it explains the AL-ADiN multifragmentation data [5] at relativistic energies quite nicely.

III. CALCULATIONS AND COMPARISON WITH DATA

We simulate the reactions of Au (35 MeV/A)+Au at six peripheral geometries using the MST and SACA methods. A *soft* equation of state ($\kappa = 200$ MeV) along with standard energy dependent n-n cross section was used for the simulation of HI reactions.

Figure 1 displays the average density reached in the reaction along with the evolution of the heaviest fragment A^{max} and multiplicity of clusters with mass A > 5 followed till 300 fm/c. One can see that as the nucleon density saturates after violent phase, SACA method is able to identify asymptotic size of the heaviest fragment A^{max} around 100 fm/c. The QMD+MST approach, on other hand, fails to detect the heaviest fragment A^{max} even at 300 fm/c. The heavier A^{max} detected with MST method at $100 \, \mathrm{fm/c}$ implies that it still assumes smaller fragments as constituents of A^{max} , being very closely spaced. We shall show later on in 3-D space that this A^{max} in actual consists of bunch of smaller clusters. The higher multiplicity of fragments with mass A≥5 obtained using SACA method (see figure 1c) clearly shows that A^{max} detected in the MST approach is actually a bunch of smaller fragments. As shown in Ref. [21], different clusterization approaches converge to same configuration at 1000 fm/c. It is, however improper to follow the reaction till 1000 fm/c with semi-classical theory, when nuclei are found to emit fraction of nucleons even after 100 fm/c.

In figure 2, we explore the sensitivity of fragment charge distribution towards clusterization algorithms. We display here the calculations using MST and SACA approaches for unfiltered events along with experimental charge yields (shown as solid circles) obtained from the decay of the quasiprojectile (QP) [17]. Top and bottom panels show the comparison of model predictions with experimental data in the impact parameter intervals $0.5 < b/b_{max} \le 0.6$ and $0.6 < b/b_{max} \le 0.7$, respectively. The MST method clearly predicts larger production probability for heavier charges. This method fails

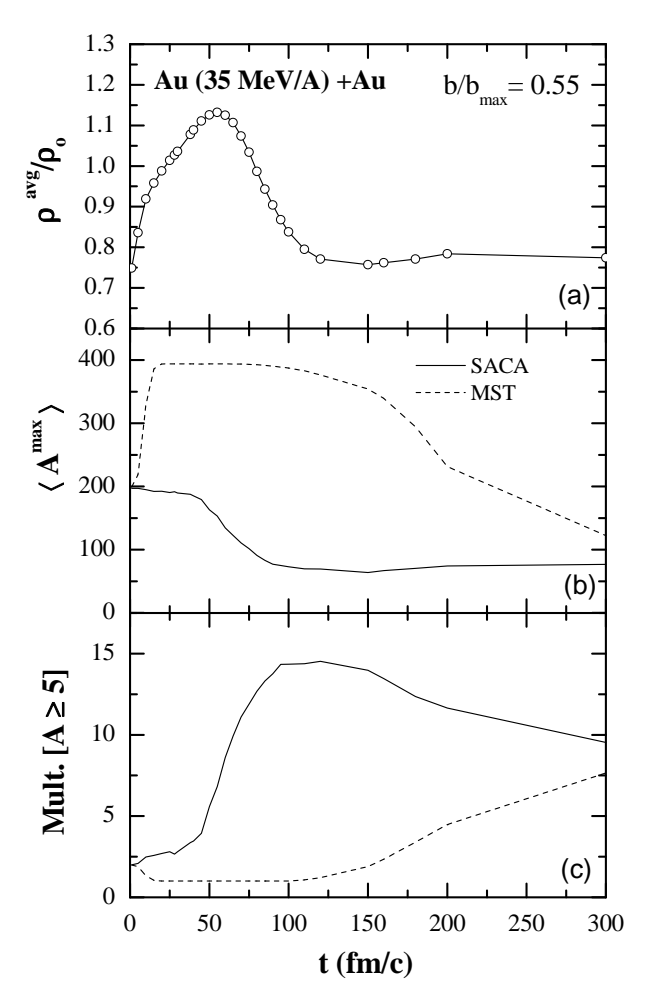


FIG. 1. The time evolution of (a) mean nucleonic density ρ^{avg}/ρ_o ; (b) size of the heaviest fragment A^{max} ; and (c) the multiplicity of clusters with mass $A \geq 5$. We display the reaction of Au(35 MeV/A)+Au at reduced impact parameter $b/b_{max} = 0.55$; $b_{max} = 1.142[A_T^{-1/3} + A_P^{-1/3}]$.

to break-up the spectator matter into smaller fragments, therefore leading to overestimated charge of heavier fragments even at $300~\rm fm/c$. As a result, the tail of charge spectrum shifts towards the higher Z values with MST method. This also highlights the discrepancy in MST procedure to describe the spectator fragmentation using semi-classical transport method. The origin of the fragments with SACA method is, however, quite earlier determined when nuclear matter is still excited and compact.

To derive quantitative information on the phenomenon of stopping, one needs to study distribution of fragments in velocity space. We display in Fig. 3, the longitudinal rapidity distributions for light charged particles LCPs $[2 \le A \le 4]$ and intermediate mass fragments IMFs $[5 \le A \le 65]$ emitted in reaction of Au(35)

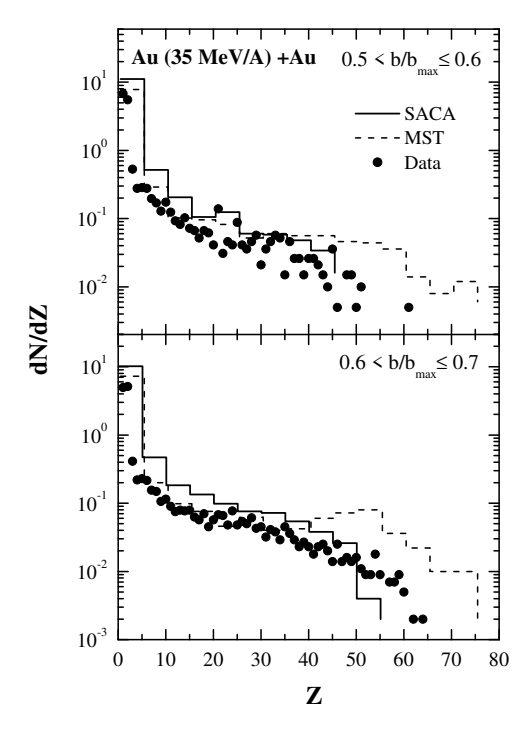


FIG. 2. The charge dispersion of the nuclear fragments in peripheral Au (35 MeV/A)+ Au collisions in the impact parameter interval $0.5 < b/b_{max} \le 0.6$ (top) and $0.6 < b/b_{max} \le 0.7$ (bottom). The model calculations using the MST (dotted curve, 300 fm/c) and SACA (solid curve, 100 fm/c) approaches are compared with the experimental data (filled circles) [17].

MeV/A)+Au at $b/b_{max} = 0.55$. Interestingly, we find that the MST method predicts the fragment-emission from mid-rapidity zone only (as indicated by a peak around $(y/y_{beam})_{cm} = 0$). SACA approach, on the other hand, indicates significant contribution coming from the target-like and projectile-like remnants apart from the mid-velocity emission. MST method can't cause cause effective break-up of spectator components to generate the IMFs close to the target and projectile rapidities even at peripheral geometries. This reflects non-equilibrium situation in the fragmenting system with SACA approach. The emission of the LCPs and IMFs near the projectile and target velocities reflects essentially the binary character of the collisions, apart from the midrapidity source emission. The peaks observed at the target and projectile rapidities is also indicative of dynamical scenario of multi-fragment emission where system has not enough time to pass through a state of thermodynamical equilibrium. It is worth mentioning that Ca+Ca collisions at 35 MeV/A were studied recently within antisymmetrized molecular dynamics (AMD) model [25]. Fragment observables such as transverse kinetic energy of fragments and radial size of the reaction system are observed to

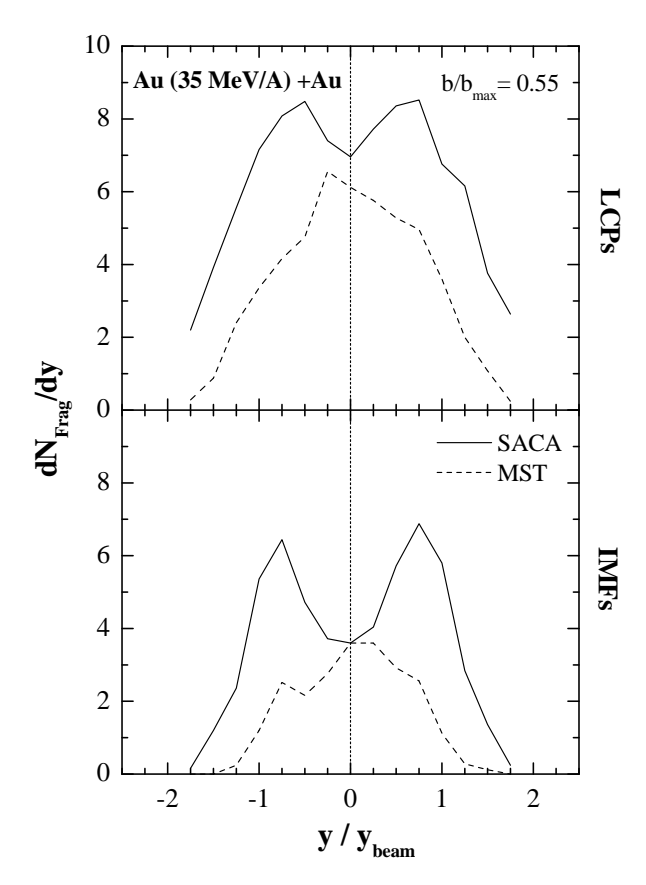
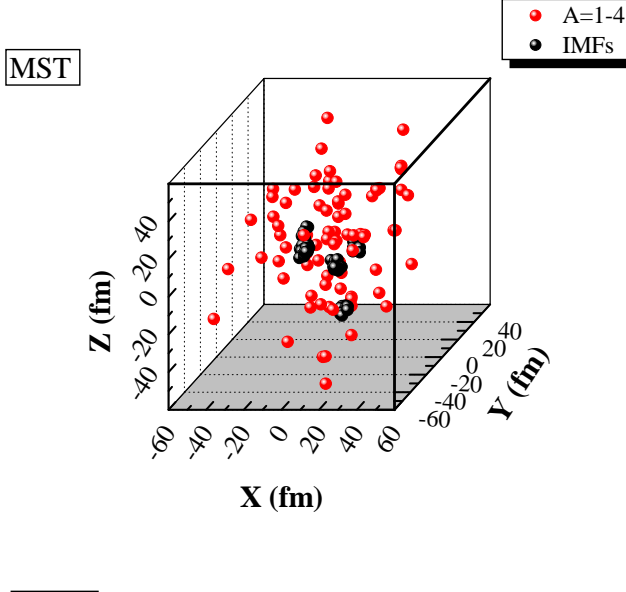


FIG. 3. The longitudinal rapidity distribution dN_{Frag}/dy of LCPs (top panel) and IMFs (bottom panel) observed in the reactions of Au (35 MeV/A)+Au at a reduced impact parameter of $b/b_{max}=0.55$. Our calculations are performed within MST (dotted curve) and SACA (solid curve) approaches.

deviate appreciably from the assumption of equilibrium ensemble. This study also favored dynamical scenario of fragmentation.

Next, we turn to the cluster distribution obtained using MST and SACA approaches in three-dimensional (3-D) coordinate space. Figure 4 displays the 3-D snapshots of cluster distribution obtained in a single event of Au(35 MeV/A) + Au collision at $b/b_{max} = 0.55$. In the MST method, free nucleons and LCPs $[2 \le A \le 4]$ are abundantly scattered in the whole space (shown as red spheres) indicating their isotropic emission from the participant zone. Only a small fraction of intermediate mass fragment IMFs $[5 \le A \le 65]$ can be seen coming out of the central overlap region. On the other hand, a significant enhancement in the production of IMFs is clearly visible for spectator zones using the SACA picture. The contribution towards the IMFs doesn't seem to come from any specific region. In other words, the QMD + SACA calculations suggest that IMFs originate from



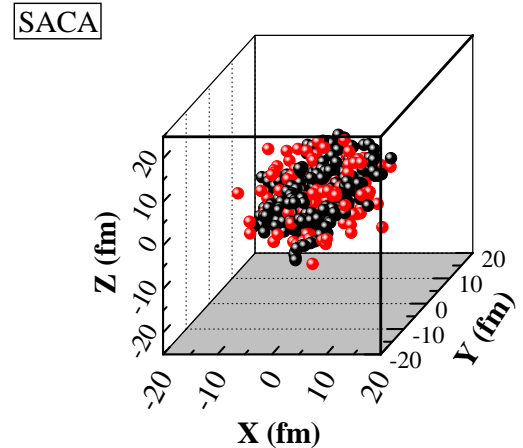


FIG. 4. (Colored online) 3-D snapshots of a single event of Au (35 MeV/A) + Au at $b/b_{max} = 0.55$ using MST (top) and SACA (bottom) pictures. Black spheres represent the nucleons distribution in IMFs and red spheres represent the nucleons distribution in clusters with mass A = 1 - 4.

the 'extended neck' region as well as from the spectator zones. The MST approach fails to break the spectator components efficiently, thereby under-estimate the IMF yields. These results highlight the importance of clustering criterion in describing reaction mechanism in low energy domain of HI reactions.

Taking the advantage that SACA approach is able to reproduce the experimental charge yields quite accurately, we further compare mean charge of the heaviest fragment $\langle Z^{max} \rangle$ obtained using MST and SACA methods with data. Figure 5 shows the mean charge of heaviest fragment $\langle Z^{max} \rangle$ as a function of 'reduced' impact parameter b/b_{max} for Au (35 MeV/A)+Au reactions. The

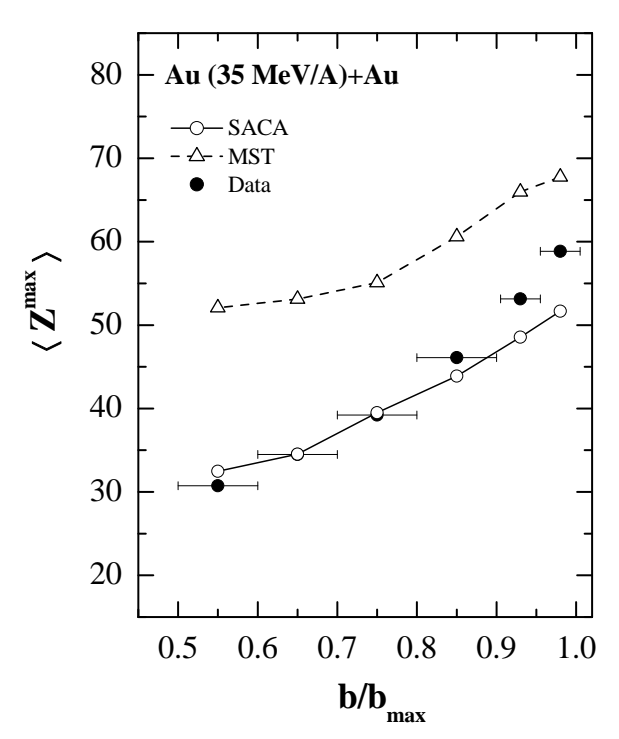


FIG. 5. The charge of the heaviest fragment $\langle Z^{max} \rangle$ as a function of the reduced impact parameter b/b_{max} . Our calculations employing the MST (dotted curve) and SACA (solid curve) approaches are compared with experimental data (filled circles) [18].

model predictions using SACA (at 100 fm/c) and MST (at 300 fm/c) approaches are displayed along with experimental data taken with combined Multics-Miniball (MM) array [18]. One can see an increasing trend of Z^{max} with impact parameter as is expected due to increase in size of spectator zone in the exit channel. Here also, QMD+MST approach fails to break the spectator matter effectively, and therefore leads to overpredicted Z^{max} even at 300 fm/c. The SACA method, on other hand, reproduces the experimental trend quite accurately at an earlier time. From these finding, we can infer that the SACA method is on reliable footing to explore the dynamics of spectator matter fragmentation in low energy

heavy-ion collisions. Further it allows faster recognition of clusters on reaction time scale.

IV. SUMMARY

Summarizing, we have performed a comparative study of two different clusterization models by simulating the peripheral $^{197}Au + ^{197}Au$ collisions at 35 MeV/A. Our calculations within QMD approach coupled with SACA clusterization subroutine showed that spectator zones contribute significantly towards fragment production in peripheral HI collisions. Contrary to this, the MST method could predict fragment-emission from mid-velocity source only even at 300 fm/c after the initial contact between projectile and target nuclei. This questions the validity of employing MST method of clusterization to investigate reaction dynamics at low incident energies. Our model predictions using the SACA method reveal that significant contribution towards IMFs emission is located near the initial target and projectile rapidities. Our model predictions for the charge distribution and mean charge of heaviest fragment $\langle Z^{max} \rangle$ using the SACA method are in nice agreement with experimental data taken with Multics-Miniball (MM) array [17, 18]. These findings highlight the importance of clustering criterion in describing mechanism behind low-energy spectator fragmentation. The SACA formalism can, therefore, be treated as general improvement over conventional clusterization algorithm to recognize the fragment structure at low and intermediate energies.

ACKNOWLEDGMENTS

One of the authors (Y. K. V) is thankful to Drs. M. Bruno and M. D' Agostino at I N F N, Italy for constructive discussions and interest shown. The research grant from Department of Science and Technology, Government of India vide grant no. SR/S2/HEP-28/2006 is gratefully acknowledged.

^[1] C. A. Ogilvie et al., Phys. Rev. Lett. 67, 1214 (1991).

M. Begemann-Blaich et al., Phys. Rev. C 48, 610 (1993);
 W. Müller, M. Begemann-Blaich and J. Aichelin, Phys. Lett. B 298, 27 (1993).

^[3] P. Kreutz *et al.*, Nucl. Phys. A **556**, 672 (1993).

^[4] J. Pochodzalla et al., Phys. Rev. Lett **75**, 1040 (1995).

^[5] A. Schüttauf et al., Nucl. Phys. A 607, 457 (1996).

^[6] A. Le Fèvre and J. Aichelin, Phys. Rev. Lett. 100, 042701 (2008).

^[7] Y. K. Vermani and R. K. Puri, Europhys. Lett. 85, 62001 (2009).

^[8] M. B. Tsang et al., Phys. Rev. Lett. **71**, 1502 (1993).

^[9] M. Colonna et al., Nucl. Phys. A 583, 525 (1995).

^[10] E. J. Garcia-Solis and A. C. Mignerey, Phys. Rev. C 54, 276 (1996).

^[11] T. K. Nayak et al., Phys. Rev. C 45, 132 (1992); B. H. Sa, R. H. Wang, X. Z. Zhang, Y. M. Zheng and Z. D. Lu, Phys. Rev. C 50, 2614 (1994).

^[12] J. J. Molitoris, H. Stöcker and B. L. Winer, Phys. Rev. C 36, 220 (1987).

^[13] M. Berenguer et al., J. Phys. G: Nucl. Part. Phys. 18, 655 (1992).

- [14] J. Aichelin, Phys. Rep. 202, 233 (1991); Ch. Hartnack et al., Eur. Phys. J. A 1, 151 (1998).
- [15] J. Péter et al., Nucl. Phys. A 593, 95 (1995); J. Toke et al., Phys. Rev. Lett. 75, 2920 (1995); R. Bougault et al., Nucl. Phys. A 587, 499 (1995); Ph. Eudes, Z. Basrak and F. Sébille, Phys. Rev. C 56, 2003 (1997).
- [16] M. Papa, T. Maruyama and A. Bonasera, Phys. Rev. C 64, 024612 (2001).
- [17] M. D'Agostino et al., Nucl. Phys. A 650, 329 (1999).
- [18] M. D'Agostino and M. Bruno, private communication.
- [19] S. W. Huang et al., Prog. Part. Nucl. Phys. 30, 105 (1993); R. K. Puri et al., Nucl. Phys. A 575, 733 (1994);
 Sanjeev Kumar, S. Kumar and R. K. Puri, Phys. Rev. C 81, 014601 (2010).
- [20] R. K. Puri, Ch. Hartnack and J. Aichelin, Phys. Rev. C 54, R28 (1996); R. K. Puri and J. Aichelin, J. Comput.

- Phys. 162, 245 (2000).
- [21] J. Singh and R. K. Puri, J. Phys. G: Nucl. Part. Phys. 27, 2091 (2001).
- [22] Y. K. Vermani, J. K. Dhawan, S. Goyal, R. K. Puri and J. Aichelin, J. Phys. G: Nucl. Part. Phys. 37, 015105 (2010).
- [23] A. D. Sood and R. K. Puri, Int. J. Mod. Phys. E 15, 899 (2006); Y. K. Vermani, S. Goyal and R. K. Puri, Phys. Rev. C 79, 064613 (2009).
- [24] T. C. Awes et al., Phys. Rev. C 24, 89 (1981); D. Fox et al., Phys. Rev. C 38, 146 (1988).
- [25] T. Furuta and A. Ono, Phys. Rev. C 79, 014608 (2009);Nucl. Phys. A 834, 555c (2010).